CZECH TECHNICAL UNIVERSITY IN
PRAGUE

Faculty of Nuclear Sciences and Physical
Engineering

Department of Physics

Bachelor thesis

HEAVY QUARK PRODUCTION ON ATLAS AT LHC

Markéta Sedláčková

Supervisor: Prom. fyz. Václav Vrba, CSc.

Prague, 2012

ČESKÉ VYSOKÉ UČENÍ TECHNICKÉ V PRAZE
FAKULTA JADERNÁ A FYZIKÁLNĚ INŽENÝRSKÁ
PRAHA 1 - STARÉ MĚSTO, BŘEHOVÁ 7 - PSČ 115 19

Katedra: fyziky   *Akademický rok:* 2011/12

ZADÁNÍ BAKALÁŘSKÉ PRÁCE

Posluchač: Markéta Sedláčková

Obor: Jaderné inženýrství

Zaměření: Experimentální jaderná fyzika

Název práce: Studium produkce těžkých kvarků pomocí ATLAS na LHC.

Název práce: Heavy quark production on ATLAS at LHC.
(anglicky)

Osnova:

Věcný obsah:
  1. Aktuální otázky výzkumu ve fyzice elementárních částic.
  2. Dráhové a mionové detektory aparatury ATLAS.
  3. Simulační a analyzační software ATHENA.
  4. Studium proton-protonových srážek s produkcí mionů.
  5. Shrnutí a závěr.

Práce bude vypracována v anglickém jazyce.

Doporučená literatura:

1. Perkins, D.H., Introduction to high-energy physics, 2000
2. Detector and physics performance, Technical Design Report Vol. 1 & 2, 1999
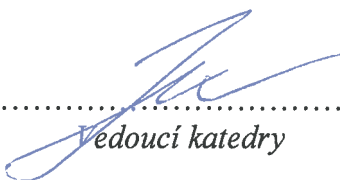3. Aktuální informace na webovských stránkách experimentu ATLAS

Jméno a pracoviště vedoucího bakalářské práce:

prom. fyzik Václav Vrba, CSc., Fyzikální ústav AV ČR, v.v.i.

Do bakalářské práce se vkládá zadání a dále na stranu předcházející obsahu abstrakt a klíčová slova. Součástí zadání bakalářské práce je její uložení na webové stránky katedry fyziky a zaslání abstraktu a klíčových slov ve formátu WORD na e-mailovou adresu katedry fyziky: kf@fjfi.cvut.cz

Datum zadání bakalářské práce: 14.10.2011

Termín odevzdání bakalářské práce: 09.07.2012

....
Vedoucí katedry   *Děkan*

V Praze dne 14.10.2011

Prohlášení:

Prohlašuji, že jsem svou bakalářskou práci vypracoval samostatně a použil jsem pouze podklady (literaturu, software, atd.) uvedené v přiloženém seznamu.

Nemám závažný důvod proti užití tohoto školního díla ve smyslu 60 Zákona .121/2000 Sb., o právu autorském, o právech souvisejících s právem autorským a o změně některých zákonů (autorský zákon).

V Praze dne

Title:
Heavy quark production on ATLAS at LHC

Author: Markéta Sedláčková

Specialization: Experimental nuclear physics

Sort of project: Bachelor thesis

Supervisor: Prom. fyz. Václav Vrba, CSc.
Consultant: Ing. Michal Marčišovský

Abstract: The first chapter of this thesis serves as an introduction to the particle physics and Standard Model. A deeper explanation of physics of b quarks, their production mechanisms and J/ψ decay channels is given. In the second chapter CERN and the ATLAS experiment are described. The construction of the detector, TDAQ and the ATLAS software framework, ATHENA, are also discussed in detail. The data analysis in third chapter revolves around J/ψ, bound state of $c\bar{c}$ quarks, which is easily identifiable in the detector in its dimuon decay channel. It is used for detector performance evaluation as well as for physics measurements. B hadrons decaying into J/ψs can be easily identified and partially reconstructed. Their angular correlations are studied in this thesis.

Work presented in this thesis is a preparation for the analysis performed in the Prague B-physics group which concerns b quark production mechanisms.

Key words: J/Psi, angular correlations, ATLAS, quarkonia, Standard Model

Název práce:

Studium produkce těžkých kvarků pomocí ATLAS na LHC

Autor: Markéta Sedláčková

Abstrakt: První kapitola této práce slouží jako úvod do částicové fyziky a do Standardního modelu. Hlubší vysvětlení je poskytnuto u fyziky b kvarků, jejich produkčních mechanismů a rozpadů J/ψ. V druhé kapitole jsou popisovány CERN a experiment ATLAS. Dále jsou zevrubně popsány konstrukce detektoru, TDAQ a ATLASovský framework, ATHENA. Analýza dat ve třetí kapitole se zábývá J/ψ, vázaným stavem $c\bar{c}$ kvarků, které je v detektoru snadno identifikovatelné svým dimionovým rozpadem. Využívá se jak ke kontrole výkonu detektoru tak k fyzikálním měřením. B hadrony rozpadající se na J/ψ jsou snadno identifikovatelné a rekonstruovatelné. V této práci jsou analyzovány jejich úhlové korelace.

Analýza presentovaná v této práci slouží jako příprava na analýzu prováděnou v pražské skupině B-fyziky, která se zabývá produkčními mechanismy b kvarku.

Klíčová slova: J/Psi, úhlové korelace, ATLAS, kvarkonia, Standardní Model

Acknowledgement

Contents

List of Figures

List of Tables

Chapter 1

The Standard Model

The aim of this chapter is to introduce the reader to the elementary particle physics. It is nowadays represented by the Standard Model, a theory which will be explained later in this chapter. Particle physics studies what the world is made of on the finest level – smaller than atoms, even smaller than protons and neutrons that form nucleus. Main sources for this chapter were books [1], [2] and [3].

1.1   Brief history of particle physics

In this section a brief history of particle physics from ancient greeks until the discovery of quarks will be presented.

From the very beginning humans believed that the world is composed of some elements and tried to discover and define them – ancient Greeks believed them to be Earth, Wind, Water, and Fire. The need to define only one elementary structure, from which everything constitutes, can be – for example – found in the work of Anaximenes of Miletus, who claimed this structure to be Air. In his works he described how other elements were obtained through condensation of the Air – more condensed gives Water and Earth, less condensed forms Fire. Another philosophical school of thought, atomism, believed that the world consists of an indivisible atom and empty void. According to Aristotle, atoms move through the void, bouncing off each other, sometimes forming a cluster. Clusters then add up, forming macroscopic structures.

However, these philosophical questions have nothing to do with modern science therefore the history of the elementary particle physics (as we know it today) starts in 1897, when J.J. Thomson discovered the electron through his explorations of the properties of cathode rays. Thomson correctly guessed that electrons are parts of atoms, and he proposed a model of atom in which negatively charged point-like electrons are flowing in a thick paste of positive charge, like the plums in a pudding (as he put it). This model ensured neutrally charged atom and solved the problem of atom being much heavier than electron. But

Thomson's model of the atomic structure was dismissed in 1911 because of E. Rutherford's scattering experiment, in which a beam of α-particles is fired into a thin sheet of gold foil. To confirm Thomson's model, all α-particles would have to pass through the sheet but in reality some bounced off at wild angles suggesting that there is something very small (occupying only a tiny fraction of the volume of the atom), very hard, and very heavy in the center of atoms. This positively charged core was called nucleus. The nucleus of the lightest atom, hydrogen, was called proton. In 1932 J. Chadwick discovered neutron – an electrically neutral twin to proton. This discovery explained the relationship between atomic mass and atomic number. Another important discovery happened in 1932 – Carl D. Anderson discovered positron (antielectron): a positively charged twin to electron. This discovery was the first evidence of antimatter – there were more eventually, in fact, every particle has its antiparticle with the same attributes except charge. The antiproton was first discovered at the Berkeley Bevatron in 1955, and antineutron was first observed at the same facility the following year.

The discovery of photon, the quantum of light and all other forms of electromagnetic radiation, was supported by theoretical predictions. At the beginning of 20th century it was believed that light is a wave (Maxwell's wave theory). However, while studying the blackbody radiation, Max Planck suggested that electromagnetic radiation is quantized and energy E is an integer multiple of radiation with frequency ν: $E = h\nu$, where h is Planck's constant. In 1905 Albert Einstein used light quanta in his explanation of photoelectric effect. He was also the first to propose that energy quantization was a property of electromagnetic radiation itself. This idea was not widely accepted until Compton's scattering experiment in 1923.

Neutrinos were first introduced to fulfil the law of conservation of energy in beta decay in 1930. They were experimentally confirmed in 1956 by Cowan and Reines who set up "inverse" beta decay reaction: $\nu_e + p \rightarrow n + e^+$ (antineutrino and proton goes to neutron plus positron). Both neutron and positron can be detected and the coincidence of both events – positron annihilation and neutron capture – gave a unique sign of an antineutrino interaction.

In 1968, deep inelastic scattering experiments at the Stanford Linear Accelerator Center (SLAC) showed that the proton itself consists of smaller objects, and therefore isn't an elementary particle itself. The idea of quark model was known at that time – in 1961 Gell-Mann introduced his particle classification system including quarks – but wasn't widely accepted, so the little point-like objects in the proton were given the name "partons". Eventually the quark theory proved to be correct and the name parton now describes "a quark or a gluon".

1.2 Interactions

There are four fundamental interactions that describe how all particles interact with each other. Their list and corresponding mediating bosons is shown in

Table 1.1.

Force	Mediator	Range	Relative Strength
Strong	Gluon	$\leq 10^{-15}$ m	~ 1
Electromagnetic	Photon	∞	$\sim 10^{-2}$
Weak	W and Z	10^{-18} m	$\sim 10^{-7}$
Gravitational	Graviton	∞	$\sim 10^{-39}$

Table 1.1: List of the four fundamental interactions. [1]

Gravitation

The weakest of all, gravity is an interaction that attracts figures with a force proportional to their mass. It is the force behind planets keeping their orbits around Sun, Moon around Earth or simply people not falling off the Earth and not floating around. However on the particle physics scale its display becomes negligible compared to the other forces, which then leads to an actual omitting gravity from elementary particle physics. A physical theory describing gravity is (classical) Newton's law of gravity and Einstein's general theory of relativity. Widely accepted quantum theory of gravity has yet to be found. Graviton is a hypothetical particle of no mass and no charge with spin 2 that mediates the gravitational force.

Electromagnetic interaction

This interaction acts between electrically charged particles and can be completely described by the Lorentz force law or Maxwells' equations. It causes atoms and molecules to hold together by binding positively charged nuclei to negatively charged electrons. Moreover, it is responsible for everything visible with human eyes – light and other electromagnetic radiation, magnetism and electricity and most of mechanics (except for gravity) are all caused by this interaction. Quantum electromagnetic theory is called quantum electrodynamics (QED), comes from 1940s and employs the photon as a mediating particle (vector boson).

Weak interaction

Weak force inherited its name from the fact that it seems weak compared to the strong or electromagnetic interaction. It is the only interaction capable of changing one type of quark into another (i.e., changing their flavour). Most common example is beta decay, in which one *down* quark changes to *up* quark. It is also responsible for decay of muons. It violates parity and even CP symmetry. The carriers of this interaction are $W^{\pm}$ and Z bosons, very heavy particles that are causing the relative slowness and short range of this interaction.

Electroweak interaction

This is a theory which unifies the weak and electromagnetic interaction be-

tween elementary particles. It is also known as Glashow-Weinberg-Salam (GWS) theory. These two interactions seem different at low energies, but above the unification energy (on the order of 100 GeV) they merge into one. The electroweak theory was suggested in 1960s and it has been experimentally verified in 1973 (discovery of the neutral currents) and 1982 (discovery of the W and Z bosons). It incorporates the Higgs mechanism in order to generate masses for the heavy vector bosons and predicts existence of the scalar Higgs boson.

Strong interaction

Strong force not only holds quarks together in hadrons, but higher momenta of the strong force also hold together nucleons in nuclei. The theory of the strong force is called quantum chromodynamics (QCD), it emerged in the 1960s, and uses massless gluons as mediators and is nowadays best theory to describe strong interaction. Gluon is a carrier of colour charge, another quantum number that will be described later in this chapter.

1.3 Standard Model

The Standard Model (SM) is a theoretical framework describing all the currently known elementary particles – it is namely consisting of twelve elementary matter particles and their antimatter counterparts, twelve intermediating particles and a recently observed Higgs boson[1]. Standard Model can be also described as a relativistic quantum field theory of fundamental particles and interactions, which simply states that the quantum theories described in Section 1.2 are used to explain particle physics and how it works. Base symmetry of the SM is $SU(2)_L \times U(1)_Y \times SU(3)_C$, where $SU(2)_L$ denotes the weak isospin symmetry from which three weak vector bosons emerge, $U(1)_Y$ is the weak hypercharge symmetry from which photon and the Z boson emerge after mixing with the neutral component of the weak isospin bosons, and $SU(3)_C$ stands for the colour symmetry of the QCD. One important thing to note is that SM is a perturbative quantum field theory, i.e. the interactions between particles are mediated by other particles, here represented by the gauge bosons (photons, $W^{\pm}$ and Z bosons, gluons).

1.3.1 Quarks and Leptons

Elementary matter particles from which hadrons are composed of mentioned in the introduction to this section are called quarks. There are six quarks in three generations: up and down, charm and strange, top and bottom. Different types of quarks are usually denoted as flavours. As already mentioned above, to each quark there is an antiquark, which has the same properties as their respective quarks, but the electric charge has opposite sign. Basic properties of the six quarks are shown in Table 1.2. All values are taken from [2].

---

[1] As of 4 July, a new particle resembling the long-sought Higgs boson has been observed at CERN in the mass region around 126.5 GeV. [4]

Name		Mass [MeV/c^2]	Charge	Spin	I_z	C	S	T	B
Up	u	1.7 to 3.3	$+2/3$	$1/2$	$-1/2$	0	0	0	0
Down	d	4.1 to 5.8	$-1/3$	$1/2$	$+1/2$	0	0	0	0
Charm	c	1180 to 1340	$+2/3$	$1/2$	0	$+1$	0	0	0
Strange	s	80 to 130	$-1/3$	$1/2$	0	0	-1	0	0
Top	t	171200	$+2/3$	$1/2$	0	0	0	$+1$	0
Bottom	b	4130 to 4350	$-1/3$	$1/2$	0	0	0	0	-1

Table 1.2: The basic properties of quarks

The uncertainties in the masses of quarks are caused by the fact that quarks have not been observed freely floating around – they always pair up, therefore making it very complicated to measure their actual mass (in this case they have been calculated using a mass-independent subtraction scheme). All quarks carry a baryon number $B' = 1/3$, which means that three quarks form a baryon ($B' = 1$) and one quark and antiquark form a meson ($B' = 0$). Baryon number is conserved in reactions. I_z, C, S, T and B stand for flavour quantum numbers. Flavour quantum number is defined as the difference between quarks of one type and antiquarks of the same type present in a particle. Their names and definitions are as follows (u,d,c,s,t,b stand for quarks):

Isospin	$I_z = \frac{1}{2}\left((n_u - n_{\bar{u}}) - (n_d - n_{\bar{d}})\right)$		
Charm	$C = n_c - n_{\bar{c}}$	Topness	$T = n_t - n_{\bar{t}}$
Strangeness	$S = -(n_s - n_{\bar{s}})$	Bottomness	$B = -(n_b - n_{\bar{b}})$

The relation between electric charge and flavour quantum numbers is defined by the Gell-Mann–Nishijima formula:

$$Q = I_z + \frac{1}{2}Y = I_z + \frac{1}{2}\left(C + S + T + B + B'\right),$$

where Y denotes hypercharge, a number that unifies isospin and flavour into a single charge. Therefore the conservation of hypercharge implies a conservation of flavour.

The remaining six elementary fermions particles are leptons. They are again ordered in three generations: electronic, muonic and tauonic leptons and to each lepton there exists a neutrino. The naming convention for antileptons comes with a small twist – due to historical reasons antielectron was given the name positron, yet it is the only exception to the standard antimatter word formation (i.e. addition of 'anti-' prefix to the lepton's name).

Their basic properties are shown in Table 1.3 (values from [2]). L_e, L_μ and L_τ stand for leptonic family quantum numbers named respectively electronic, muonic and tauonic number. These lepton numbers are defined as the number of leptons minus the number of antileptons ($L = n_l - n_{\bar{l}}$). In the Standard Model lepton number L is conserved, moreover lepton number of each generation (L_e, L_μ and L_τ) is conserved, e.g. muon decay:

Name		Mass [MeV/c^2]	Charge	Spin	L_e	L_μ	L_τ
Electron	e^-	0.51	-1	1/2	1	0	0
Muon	μ^-	105.66	-1	1/2	0	1	0
Tau	τ^-	1776.84	-1	1/2	0	0	1
Electron neutrino	ν_e	< 0.0000022	0	1/2	1	0	0
Muon neutrino	ν_μ	< 0.17	0	1/2	0	1	0
Tau neutrino	ν_τ	< 15.5	0	1/2	0	0	1

Table 1.3: The basic properties of leptons

$$
\begin{array}{ccccccccc}
 & \mu & \rightarrow & e^- & + & \bar{\nu}_e & + & \nu_\mu \\
L: & 1 & = & 1 & - & 1 & + & 1 \\
L_e: & 0 & = & 1 & - & 1 & + & 0 \\
L_\mu: & 1 & = & 0 & + & 0 & + & 1
\end{array}
$$

1.3.2   Particle Classification

It has been previously mentioned that quarks cannot be found alone on their own but they "team up". This section will help with classification of what particles can be found (or formed).

Fermions   are particles that obey Fermi-Dirac statistics and follow Pauli exclusion principle. They have half-integral spin. In the Standard Model they are represented by quarks and leptons.

Bosons   are the other fundamental class of subatomic particles. Bosons obey Bose-Einstein statistics, have integer spin and are represented by interaction particles. The four gauge bosons (photon, W$^\pm$, Z and gluon) have spin one, Higgs boson, that should give masses to intermediating bosons as well to all other weakly interacting particles, has zero spin and the gravity force carrier, graviton, is suggested to have spin 2.

Subset of fermions – leptons – has been already described in the previous section. The basic properties of quarks were also written there but unlike leptons quarks form themselves into compound forms called *hadrons* that are further divided in two groups:

Baryons   are bound states of three quarks qqq (or three antiquarks $\bar{q}\bar{q}\bar{q}$), therefore their baryon number is $B' = 1$ (or -1). The observed existence of baryon consisting of three quarks of the same flavour (e.g. $\Omega^-(sss)$ with spin 3/2) seems to violate the Pauli exclusion principle. This problem was solved by adding a new quantum number called colour charge, which is studied in the QCD. All baryons except proton are unstable.

Mesons are bound states of quark q and antiquark $\bar{q}$ with baryon number $B' = 0$. They are all unstable. Because of their lower mass (in relation to baryons) it is easier to create them in accelerator experiments, which then can lead to the discovery of new flavours. For example, the discovery of J/Ψ meson, consisting of c and $\bar{c}$ quark in 1974 lead to the discovery of the charm quark.

These two categories of hadrons are not the only ones theoretically possible, yet they are the only ones observed. The theory permits creation of so called exotical particles: tetraquarks ($qq\bar{q}\bar{q}$), pentaquarks ($qqqq\bar{q}$) or glueballs (gg). However, to explain theoretically predicted possibility of their existence is beyond capacity of this thesis.

1.3.3 Eightfold Way

Elementary particles can be organized into various geometric shapes based on their charge and strangeness. This, in fact, led to the discovery and final acceptance of the quark theory – in 1964 Murray Gell-Mann proposed an Eightfold Way, a theory organizing subatomic baryons and mesons into multiplets, starting with the meson octet that can be seen in Fig. 1.1. Particles along the same horizontal line share the same strangeness S while those on the same diagonals share the same charge q. Not only hexagons are used which can be seen in Fig. 1.2 which is a triangular array. When Gell-man was forming the decuplet, one particle was missing – the one in the bottom row, now recognised as Ω^-. Gell-Mann predicted its existence, calculated its mass and lifetime, and told the experimentalists how to produce it. In 1964 Ω^- was discovered with exactly the same properties as predicted. Ever since, nobody really doubted the Eightfold way and more multiplets were formed (one more can be found in Fig. 1.3).
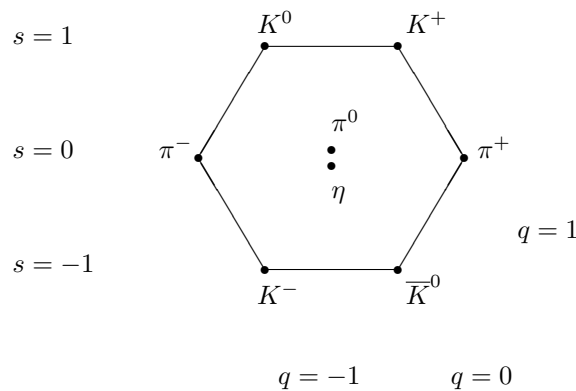

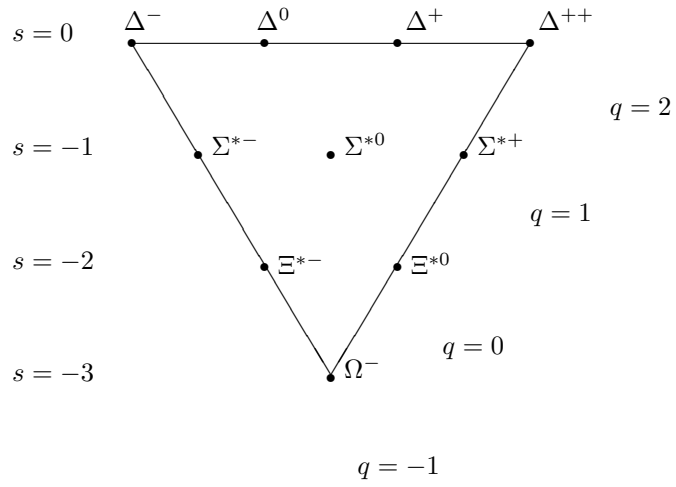Figure 1.1: Meson octet, part of the Eightfold way. Figure from [5]

Figure 1.2: Baryon decuplet, part of the Eightfold way. Figure from [5]
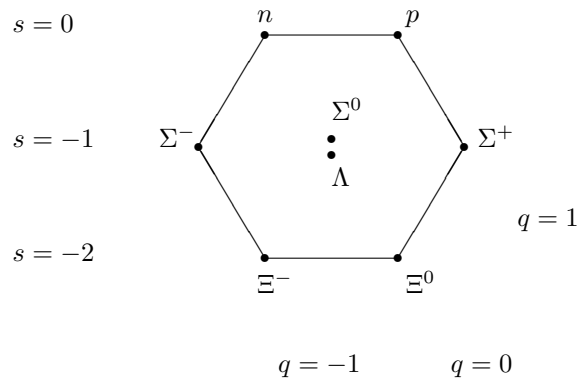

Figure 1.3: Baryon octet, part of the Eightfold way. Figure from [5]

1.3.4 Symmetries

Symmetries in physics hold a very special place – they denote invariance under any kind of transformation, which means that symmetries occurring in nature are represented by conservation laws. In the particle physics, they help to study the properties of elementary particles. An example of symmetry is parity: it is impossible to denote our universe from universe where everything appears as if reflected in a mirror.

Symmetries can be divided into two categories: *continuous* and *discrete* which will be further described later. Other classification is *global* and *local* symmetries – global symmetry works in all points of spacetime, whereas a local symmetry is one that varies at different points of spacetime.

Continuous symmetries

These symmetries are characterized by an invariance following a continuous change in the geometry of the system, mathematically they are represented by continuous or smooth functions. Spacetime symmetries involve time translation (system feature does not change with a continuous change in time), spatial translation (system feature does not change with a continuous change in location) and spatial rotation. These symmetries then form conservation laws of energy, momentum and angular momentum. Noether's theorem is fundamental for the study of continuous symmetries. It says, in principle, that if there is a continuous symmetry found in a system, then there also are corresponding quantities whose values are conserved in time.

Discrete symmetries

Discrete symmetries are denoted by non-continuous changes in a system. In particle physics Charge, Parity, and Time are discrete symmetries of great importance. C-symmetry stands for symmetry of physical laws under a charge conjugation transformation. In classical physics this symmetry is proved by the invariance of charge conjugation in Maxwell equations. However in quantum mechanics this term also indicates particle-antiparticle conjugation. Parity is an inversion of spatial coordinates $(x, y, z) \rightarrow (-x, -y, -z)$ (an example is given above). T-symmetry is represented by time reversal (direction of time is made to run backwards instead of forward). CPT theorem says that CPT symmetry is always conserved. Thus when CP violation was found in 1964 in decays of kaon, it is expected that T violation must exist. Other combinations of conservation/violation are also allowed (and observed).

Overall symmetries and conservation laws have a big role in physics. They usually make problem computations easier (through reducing the number of variables). However not all conservation laws work with all interaction – this is summed up in Table 1.4. Symbol $+$ stands for conserving and $-$ for not conserving the variables.

Variable	Strong	Electromagnetic	Weak
Energy, momentum	+	+	+
Electric charge	+	+	+
Baryon number	+	+	+
Lepton number	+	+	+
Isospin	+	−	−
CPT	+	+	+
CP (or T)	+	+	−
C	+	+	−
P	+	+	−

Table 1.4: Table of validity of conservation laws

1.3.5   SM Problems

Even though Standard Model describes vast majority of observed phenomena, it does not offer answer to everything.

First of the problem is the insufficient explanation of gravitation. Theoretical particle known as a graviton could help with incorporating it into the Standard Model, but the theory is still not thorough. Moreover SM is incompatible with the General Relativity.

The Standard Model also predicts massless neutrinos. However, recently neutrino oscillations were observed (e.g. as a solution to the solar neutrino problem), indicating that neutrinos have mass. The SM can be adjusted to include the masses, but as a proper theory it should have included them from the beginning. Mass of the neutrino can be generated for example by the see-saw mechanism. In fact, the SM only predicts existence of particles and not their masses. Also 25 numerical constants[2], whose values had to be obtained experimentally and could not be predicted theoretically, are needed to describe SM. This is way too many basic constants for any elementary theory.

Last but not least, dark matter and dark energy – an entities which make up about 24 and 72 % of the Universe respectively. They are hardly described by the SM, the dark matter is supposed to be composed of elementary particles, they are expected to be lightest supersymmetric partners of the SM particles, yet they haven't been detected as of now. Dark energy is even greater mystery, it's density is constant in time and it's proportion rises. It is expected to be the vacuum energy.

---

[2]Namely: 6 masses of quarks, 6 masses of leptons, 4 parameters of the CKM matrix (3 mixing angles and one phase - quark mixing and CP violation parameters), 4 parameters of the Pontecorvo-Maki-Nakagawa-Sakata matrix (neutrino oscillations), the fine structure constant, the strong coupling constant, the Higgs boson mass, the W boson, the Z boson and 26th is cosmological constant.

1.3.6   Beyond the Standard Model

Standard Model is not perfect and all-solving – some of its problems were described above. Thus new theories trying to solve the shortcomings rose. They are usually called "Beyond SM" and three representatives will now be introduced.

SUSY

Supersymmetry (SUSY) is a theory that extends the Standard Model by adding an additional class of symmetries which leads to the existence of the supersymmetric particles. These particles postulate a fermion-boson symmetry: to every known fundamental fermion (boson) a new boson (fermion) is presumed. These superpartners differ by spin 1/2 from the original particles and are also much heavier due to the breaking of supersymmetry (so much heavier that they could not have been detected yet). This hypothesis could solve the hierarchy problem, a (theoretical physics) situation when the fundamental parameters of some Lagrangian are vastly different than the parameters measured by experiment. In particle physics this problem for example covers the question why is the weak force 10^{32} times stronger than gravity.

String theory

In this theory elementary particles are represented as strings of finite length instead of being point-like. Their dimension is of order 10^{-35} m. The advantage of this theory is the incorporation of gravity and the diminution of parameters needed to define the theory. The downs are that at least 10 dimensions are needed to be used in order for this theory to work (four are time and space related, remaining six dimensions are curled up hence being undetectable) and that there is no experimental way how to prove whether it is correct or not. Therefore the biggest advantage of this theory up to date is that using strings makes computation of some physical problems easier.

GUT

GUT stands for Grand Unified Theory. This theory aims at the unification of interactions. Electromagnetic and weak force have already been unified in electroweak theory, which gives the scientists hope to unify even more forces together. GUT should connect electroweak with strong interaction and another theory called TOE (Theory Of Everything) should unify all known forces. Each force has its coupling constant whose values vary with energy (see Fig. 1.4). At approximately 10^{19} GeV they should become equal. The three known interactions are therefore low-energy limit of GUT. This theory is being tested – one of its prediction is that proton is not stable (though its lifetime is greater than 10^{31} years). The setting of the experiment Super-Kamiokande (Japan) consists of a huge underground chamber containing 50 000 tons of ultra-pure water 1 km underground. When the rare decay happens Cherenkov light should be seen.
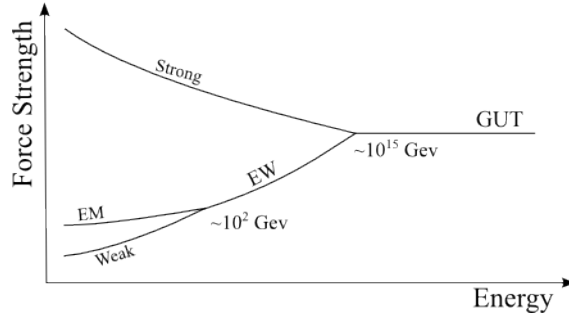
Figure 1.4: Grand unified theory and the change of coupling constants

1.4 B Physics

B Physics is a common name given to part of elementary particle physics that studies properties of the b quark. To present this part of physics, a bit deeper explanation of the strong interaction than the one given in the Section 1.2 must be done, which will be covered in this Section. Furthermore, the basic QCD b-quark pair creation mechanisms and properties of angular correlations of $b\bar{b}$ quarks will be described here. The structure of this introductory section is based on Ref. [6] and [7].

1.4.1 Strong Interaction

Strong interaction adds new quantum number called colour. The basic property of colour is as follows: Any quark can exist in three different colour states. These are called 'red', 'green', 'blue' and are simply denoted as r, g, b; to antiquarks an anticolour is assigned (antired r̄, antigreen ḡ and antiblue b̄). New quantum number adds a theorem: All naturally occurring particles must be colourless. This phenomenon is called *colour confinement*.

The initial problem from Section 1.3.2 with Ω^- that has spin $3/2$ – which means that all three like quarks have the same space and spin states – is thus solved by adding a new part to total wavefunction so that it consists of three parts: spatial part, spin part, and colour part, or mathematically:

$$\Psi = \Psi_{space}(r)\Psi_{spin}\Psi_{colour}$$

The Pauli principle is now applied on total wavefunction meaning that quarks in hadrons can exist in the same spin and spatial state due to having different colour.

The strong interaction's force carriers are gluons that couple to colour charge. Because of their nonzero values of the colour charge they couple not only with quarks but also with other gluons. The nonzero colour charge is also source of confinement of quarks. Gluons interactions in elementary interaction vertices of QCD are shown in Fig. 1.5. If the gluon-gluon interactions were attractive and
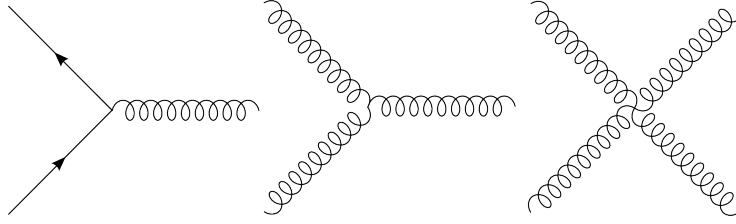
Figure 1.5: The three leading order vertices in QCD

sufficiently strong, they could form a particle consisting only of gluons. These exotic particles are called glueballs and haven't been observed yet.

Another interesting property associated with strong interaction is *asymptotic freedom* – fact that quarks interact more strongly the further they are apart, and more weakly as they are close by. The implication of this fact is a free movement of quarks within the hadrons. The strong force coupling constant is approximately one ($\alpha_s \approx 1$), but for small energies (where asymptotic freedom matters) it starts to increase rapidly.

1.4.2   Bottom quark production

Bottom quark was discovered in 1977 by the Fermilab E288 experiment. Its basic properties were described in Table 1.2. Among hadrons that bottom quark forms belong: Υ ($b\bar{b}$), B mesons (b quark with up or down quark), B_C and B_S mesons (b plus charm or strange quark) and bottom baryons.

Bottom quark production happens mostly through strong interaction. The leading order (LO) production mechanism is *flavour creation* (FCR), which is shown in Fig. 1.6. It is a $2 \to 2$ process:

$$q\bar{q} \to Q\bar{Q}, \; gg \to Q\bar{Q}$$

where Q denotes a heavy quark. The next to leading order (NLO) is characterised by two $2 \to 3$ processes. First is *flavour excitation* (FEX) and the latter *gluon splitting* (GSP). flavour excitation (shown in Fig. 1.7) can be summarised as process consisting of:

$$q\bar{q} \to b\bar{b}g, \; gg \to b\bar{b}g, \; gq \to b\bar{b}q, \; g\bar{q} \to b\bar{b}\bar{q}$$

In gluon splitting a final-state gluon splits into $b\bar{b}$ pair as schematically shown in Fig. 1.8.

Since all three processes lead to different kinematic distributions it is possible to measure their relative contributions to the total cross section in data. More on this topic will be described in Chapter 3.
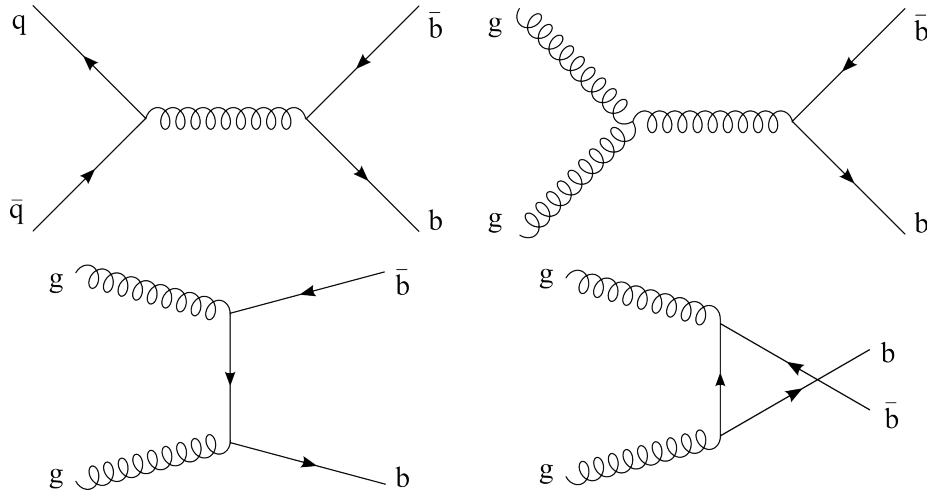
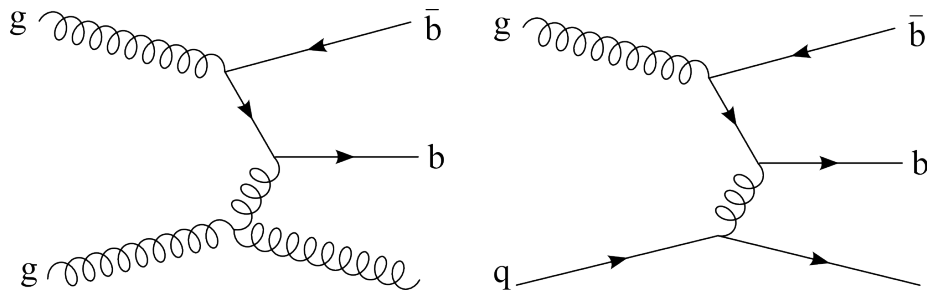Figure 1.6: Leading order $b\bar{b}$ production mechanisms

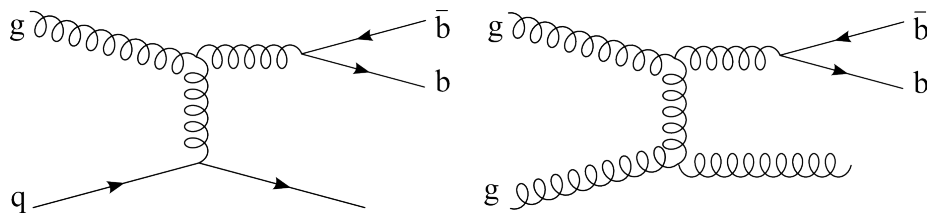Figure 1.7: The next-to-leading order $b\bar{b}$ *flavour excitation* process

Figure 1.8: The next-to-leading order $b\bar{b}$ *gluon splitting* process

Chapter 2

ATLAS Experiment

In this chapter, CERN, a place where particle physics experiments which this thesis concerns are taking place, will be briefly introduced. Moreover its collider system, of which the Large Hadron Collider (LHC) is the largest, will be presented. Chapter 3 of this thesis discusses specific data analysis done with LHC data, therefore the ATLAS detector and the software used to analyse the data will be presented. Information for this chapter comes from [8], [9], and [10].

2.1 CERN

CERN (European Organization for Nuclear Research) is the world's largest particle laboratory. Founded in 1954, it is located at the Franco-Swiss border. Particle physics experiments are happening there on a daily basis, because the particles at LHC keep colliding.

However, discoveries coming from the LHC won't be the first ones coming from CERN. One of its first discoveries came in 1973: it was the discovery of neutral currents. Weak neutral currents, reactions where the charges of the interacting particles are not shuffled around, were part of the electroweak theory from the 1960s. In 1972 an event in the Gargamelle bubble chamber happened: a neutrino passing through jolted an electron on its way. This was later confirmed as neutral currents reaction. The carriers of the weak force, charged $W^{\pm}$ and neutral Z boson were also first observed in CERN – it was in 1983 at the CERN's Super Proton Synchrotron. In 1989 the number of lepton families was set to three from study of Z decay width.

Also the CERN's study of antimatter should be mentioned. The study of matter-antimatter symmetry continues up to nowadays. In 1995 first antihydrogen atoms were observed at CERN – the first time ever when antimatter particles formed an atom. The antihydrogen atoms, when created, were flying at nearly the speed of light. To study them better, they had to be slowed down (achieved in 2002). Their observation was confirmed through their annihilation with ordinary matter.

2.2 LHC

Large Hadron Collider (LHC) is the newest particle accelerator added to the CERN's accelerator complex. It is buried from 50 to 175 m underground Franco-Swiss border. It started operating on 10 September 2008 but nine days later it stopped operating due to a magnet quench incident. On 20 November 2009 the proton beams again started to circulate and three days later the first proton–proton collisions were recorded at the injection energy of 450 GeV per beam, thus commencing the planned research program. In 2010 and 2011 it operated at beam energy of 3.5+3.5 TeV, switching to 4+4 in 2012. The LHC will operate at 4 TeV per beam until the beginning of 2013, then it will be shut down for two years to do upgrades to allow full energy operation at 7 TeV per beam.

The LHC is built in a circular tunnel 26.659 km in circumference which was previously occupied by the Large Electron-Positron Collider (LEP). The LEP was operating for 11 years (from 1989 to 2000) and in the end the beams of electron/positrons were colliding at a total collision energy of 209 GeV. Among its scientific goals and achievements were testing the Standard Model, discovering (confirming) $W^\pm$ and Z bosons mentioned above, and setting the lower limit for the possible mass of the Higgs boson.

The LHC is designed to collide protons or lead ions. It is a synchrotron, a cyclic particle accelerator where electrical field is used to accelerate particles and magnetic field is used to bend their path to keep them moving with constant radius. The collider tube contains two adjacent parallel beam pipes, since there was not enough space in the tunnel for another ring. Each pipe contains a proton beam, which travels in opposite directions around the ring. The beam pipes intersect at four points at which the experiments are located. Quadrupole magnets are used to focus the beam and dipole magnets are used to bend it.

CERN's accelerator complex is a succession of particle accelerators that boost particles to higher energies. Each of this accelerators sends the beam of particles to the next one, giving the particles higher energy. Last accelerator is the LHC with the (designed) energy of 7 TeV. The movement of a particle is determined by energy instead of velocity because in high energy accelerators particles fly near the speed of light most of the time – e.g. when particles enter the LHC (at energy 450 GeV) they are moving with the speed of 0.999 997 828c (c denotes the speed of light) whereas when they are sped up to maximum energy 7 TeV they are moving with the speed of 0.999 999 991c.

The accelerator complex is shown in Fig. 2.1. The route of the accelerated particle is as follows: firstly, protons are obtained by removing electrons from hydrogen atoms and they are injected from the linear accelerator (LINAC2) into the PS Booster, then the Proton Synchrotron (PS), followed by the Super Proton Synchrotron (SPS), before finally reaching the Large Hadron Collider (LHC). Protons circulate in the LHC for 20 minutes before reaching the maximum speed and energy. Lead ions for the LHC start from a source of vaporised lead and enter LINAC3 before being collected and accelerated in the Low Energy Ion Ring (LEIR). They then follow the same route to maximum acceleration as the protons.
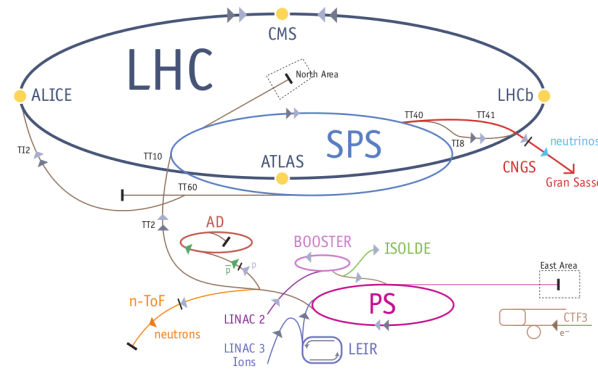
Figure 2.1: CERN's accelerator complex. Figure from [8]

LHC is not a perfect circle. In fact, it is made of eight arcs and eight straight sections. These straight sections serve different purposes: physics (experiments' caverns), injection, beam dumping, and beam cleaning, therefore their layout depends on the purpose. The arcs, however, all look the same: each contains dipole magnets used to bend the beams.

There are four major experiments (each has its own underground cavern) and two smaller ones (adjoined in caverns of other experiments) in the LHC:

ALICE (A Large Ion Collider Experiment) analyses collisions of lead ions. It aims to study properties of a state of matter known as the quark-gluon plasma, which would help to understand what was the universe like just after the Big Bang. It tries to discover unconfined quarks and gluons in QGP.

ATLAS (A Toroidal LHC Apparatus) is one of the two general-purpose detectors at the LHC. Its primary goal is to further confirm Standard Model and look for discoveries beyond it – such as Higgs boson, extra dimensions, and dark matter particles.

LHCb (Large Hadron Collider beauty) aims to study the differences between matter and antimatter. It also aims to answer the question why there was more matter over antimatter after the Big Bang. It does so through studying the b quark.

CMS (Compact Muon Solenoid) is the second one of the two general-purpose detectors at the LHC. Its has the same scientific goals as ATLAS experiment, however the technical design of the detector is different, which means that these two experiments can independently check each other's results.

LHCf (Large Hadron Collider forward) is one of two small LHC experiments. It is located on both ends of ATLAS's collision point and uses forward particles created inside the LHC as a source to simulate cosmic rays in laboratory conditions.

TOTEM (TOTal Elastic and diffractive cross section Measurement) is the other small LHC experiment. It is located in CMS's cavern. This experiment measures the effective size of the proton at LHC and also accurately monitors the LHC's luminosity.

Besides these LHC experiments, CERN holds also non-LHC ones. For example, at the SPS the COMPASS experiment is studying how the elementary quarks and gluons work together to form observed particles. NA61/SHINE is studying properties of the production of hadrons. NA62 uses protons from the SPS to study rare kaon decays. At the Proton Synchrotron DIRAC is studying the strong interaction in depth. CLOUD experiment is investigating a possible link between cosmic rays and cloud formation. Last but not least, at the Antiproton Decelerator AEgIS studies a gravitational effect on an antihydrogen, ALPHA is a neutral trap used to capture and analyse antihydrogen, ASACUSA investigates fundamental differences in the behavior of matter and antimatter, ACE is testing using antiprotons as a new cancer treatment, and ATRAP compares hydrogens' properties to antihydrogens'.

2.3   ATLAS Detector

In this section, the geometry of the ATLAS detector will be described. The detector is 46 m long with 25 m diameter and consists of four main parts: *inner detector* that measures the velocity of each charged particle, *calorimeter* that measures the energies carried by the particles, *muon spectrometer* which identifies and measures the momenta of muons, and *magnet system* which is bending charged particles for momentum measurement. The overview is shown in Fig. 2.3. A basic scheme of a particle identification in the ATLAS detector is on the Fig. 2.2. The ATLAS coordinate system is described in Section 3.1.
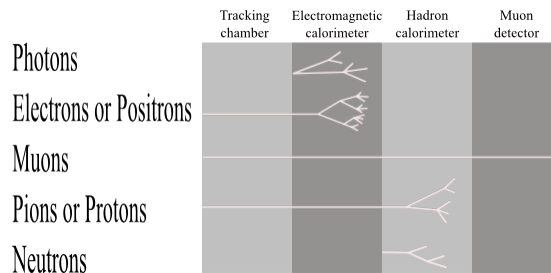

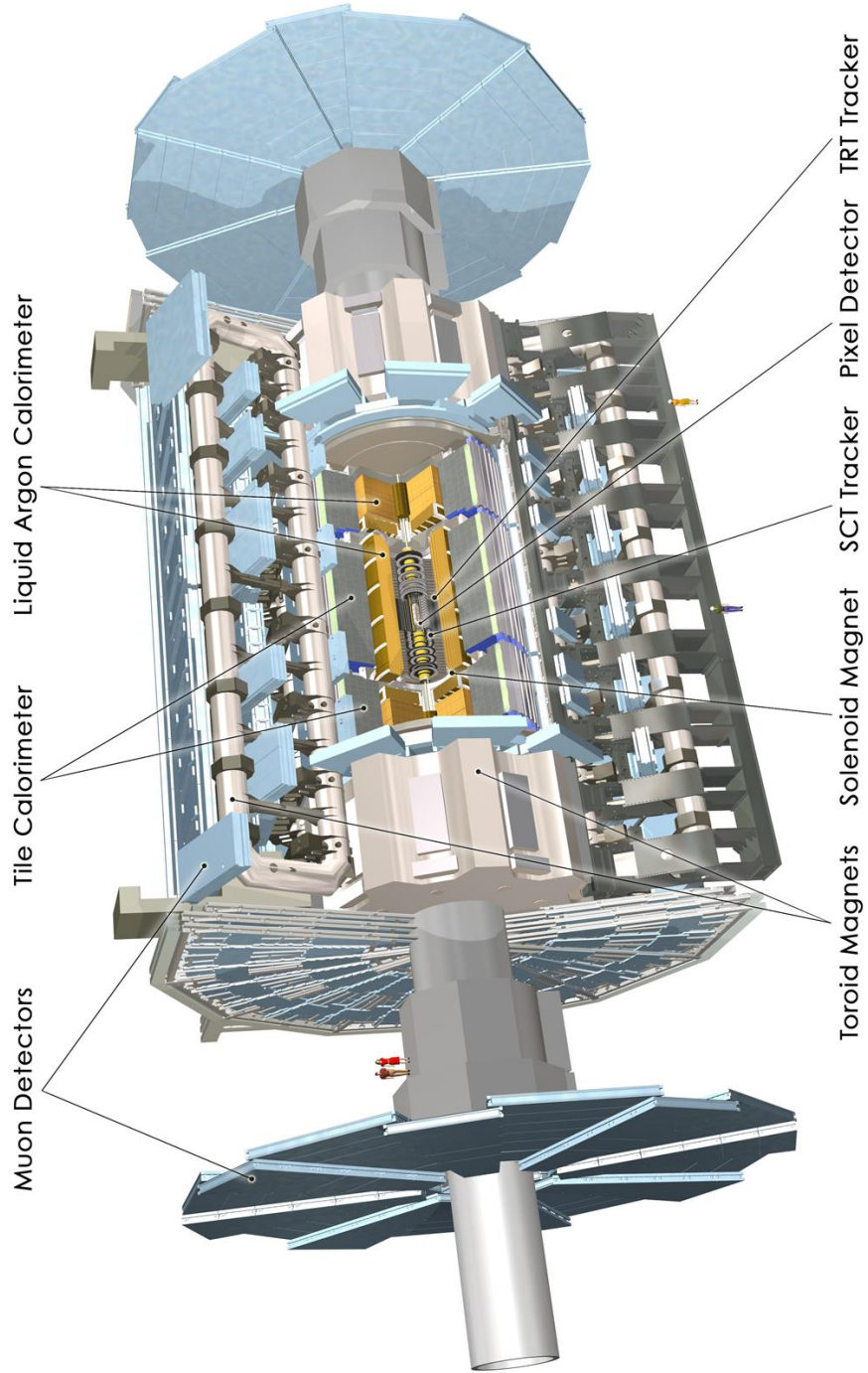Figure 2.2: A basic scheme of a particle identification. Figure adapted from [9]

Figure 2.3: The ATLAS detector. Figure from [9]

2.3.1 Inner Detector

The outer radius of the Inner Detector (schematic view shown on the Fig. 2.4) is 1.15 m, and the total length 7 m. In the barrel region the high-precision detectors are arranged in concentric cylinders around the beam axis, while the end-cap detectors are mounted on disks perpendicular to the beam axis. It has full coverage in ϕ and covers pseudorapidity range up to $|\eta| < 2.5$. The Inner Detector consists of three subsystems that are immersed in a 2 Tesla axial magnetic field:
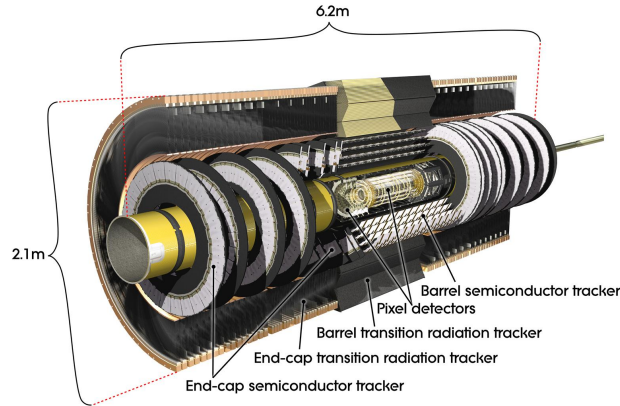
Figure 2.4: Schematic view of the ATLAS Inner Detector. Figure from [9]

Pixel Detector

It consists of 80 million pixels, which means 80 million channels to measure the information provided by particles. Size of each pixel is 50×400 μm^2. The geometry of the Pixel Detector is three barrels and three disks at every end. The system provides three precision measurements over the full acceptance.

Semiconductor Tracker

SCT is a silicon microstrip tracker designed to provide eight precision measurements per track in the intermediate radial range, contributing to the measurement of momentum, impact parameter and vertex position. It consist of 4088 two-sided modules and over 6 million implanted readout strips. It covers $|\eta| < 2.5$.

Transition Radiation Tracker

TRT is a combined straw tracker and transition radiation detector. It provides additional information on the particle type that flew through the detector. The basic detector element is a straw tube. The TRT provides on average 36 two-dimensional measurement points with 0.170 mm resolution for charged particle tracks with $|\eta| < 2.5$ and $p_T > 0.5$ GeV.

2.3.2 Calorimeters

Calorimeters measure the energies carried by the particles. In general, calorimeter consists of metal plates (absorbers) and sensing elements. In ATLAS detector there are two types of calorimeters used: In the inner section of the calorimeter Liquid Argon (LAr) calorimeter is used and in the outer section Tile Calorimeter is used. LAr uses liquid argon as the sensing element. Overall, liquid argon is used in forward calorimeter, electromagnetic and hadronic calorimeters. Tile calorimeter (consisting of 50 000 tiles) uses steel as the absorber material and scintillating plates as the active medium. It covers the central range ($| \eta | < 1.7$), as can be seen on Fig. 2.5.
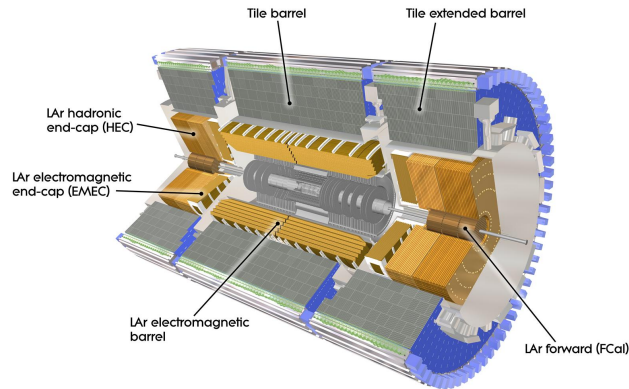

Figure 2.5: Schematic view of the ATLAS Calorimeters. Figure from [9]

2.3.3 Muon Spectrometer

The Muon System identifies and measures the momenta of muons, the only detectable particles that can traverse all the calorimeter absorbers without being stopped. It consists of main four parts, as shown on Fig. 2.6:

Thin gap chambers (TGC) are used for triggering and second coordinate measurement at the ends of detector. It consists of 440 000 channels.

Resistive plate chambers (RPC) are used for triggering and second coordinate measurement in central region. It consists of 380 000 channels.

Monitored drift tubes (MDT) measure curves of tracks. Tubes used are similar to the straws used for the Inner Detector but larger in size. It consists of 1 170 chambers.
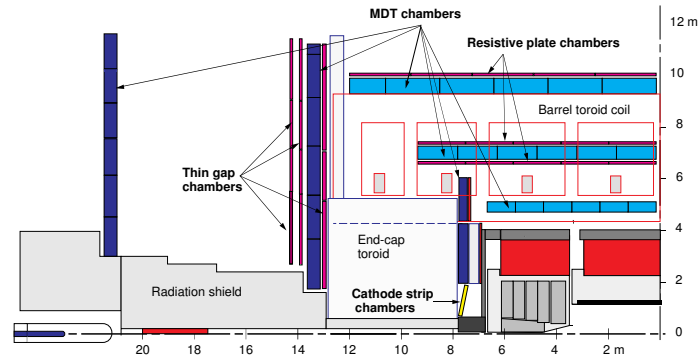
Figure 2.6: Schematic view of the Muon System at ATLAS. Figure from [11]

Cathode strip chambers (CST) measure precision coordinates at ends of detector. It consists of 70 000 channels.

2.3.4 Magnet System

Magnet System is used to bend charged particles for momentum measurement. The system consists of three sub-systems: one Barrel Toroid, two Endcap Toroids and one Central Solenoid. The Barrel Toroid covers the central region and provides some 3 - 8 Tm and consists of 8 flat superconducting race-track coils grouped in a torus shape. The forward regions are covered by two Endcap Toroids providing 3 - 8 Tm. The Central Solenoid provides 2 Tesla in the central tracking volume. Schematic view is on the Fig. 2.7.
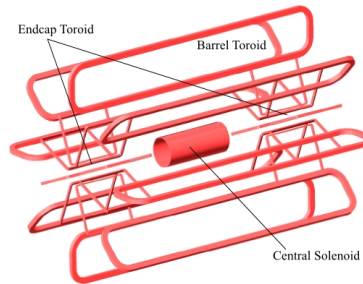

Figure 2.7: Schematic view of the ATLAS's Magnet System. Figure from [9]

2.4 ATLAS Software

All ATLAS software can be divided into two groups: *online* and *offline.* Online software is used during data collecting – it is represented by TDAQ (Trigger and Data Acquisition). Offline software is used for processing and analyzing

collected data, as well as Monte Carlo generation, detector simulation, and displaying events.

2.4.1 Trigger and DAQ

Trigger system is used in event selection, aiming not to throw out good events. The Data Acquisition system channels the data from the detectors to storage.

The TDAQ has a 3 level trigger system (an overview is shown on Fig. 2.8) used for event number reduction – in the accelerator bunches of protons cross 40 million times a second, thus incoming event rate per second is 40 000 000. Level 1 Trigger reduces this number to 100 000, which is then lowered to 3 000 by Level 2 Trigger and the final outgoing event rate per second after third reduction is 200. Total event reduction factor by the trigger system is 200 000.
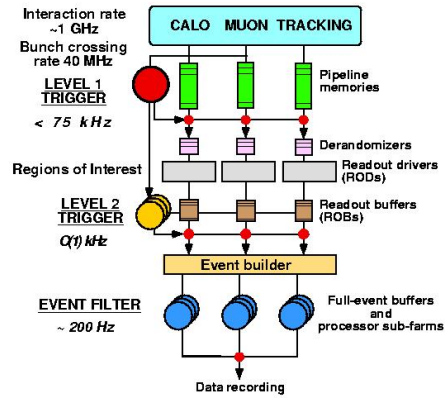

Figure 2.8: The ATLAS trigger system overview. Figure from [9]

Level 1 Trigger (LVL-1) is hardware using special-purpose processors developed and build by ATLAS collaboration. The second and third, Level 2 trigger (LVL-2) and Event filter (EF), are software based located at large computing farms (the former with approximately 500 dual pc processors and the latter with 1700).

Level 1 Trigger
The first task of the Level 1 Trigger (LVL-1) is to provide signal decision of each bunch crossing and post the data for further analysis in case of interesting event. The second function is to find RoI (Region of Interest) and post this information to the Level 2 Trigger (LVL-2). It requires about 2 micro-seconds to decide whether to keep or decline an event. The LVL-1 has two major decision branches: the muon and the calorimeter trigger. Muon LVL-1 is based on trigger detectors in muon spectrometer. The calorimeter system is based on towers (constant regions in $\eta \times \varphi$ coordinates).

High Level Trigger

High Level Trigger (HLT) is a summarizing name for LVL-2 and Event Filter (EF). The LVL-2 refines the selection of candidate objects compared to LVL-1, using full-granularity information from all detectors, including the inner tracker which is not used at LVL-1. The EF reconstructs events with online algorithms and its output is byte-stream RAW files filled with interesting event data (more on data types in next section).

2.4.2 Offline software

The ATLAS computing system is designed to analyse the data produced by the ATLAS detectors. The core of the ATLAS offline software is Athena framework, which will be briefly described. Athena covers almost everything: from skimming the data (and reducing files' volume) to plotting histograms.

Athena is a software framework, which means that it serves as a skeleton for all developed applications. It also predefines a high level 'architecture' or software organization and controls the configuration, loading and execution of the software making the end-user's work easier. It is based on C++ and is an enhanced version of the Gaudi framework that was originally developed by the LHCb experiment, but is now a common ATLAS–LHCb project – Gaudi serving as a kernel of software common to both experiments, while Athena is the sum of this kernel plus ATLAS-specific features.

Athena uses a unified hierarchy of data types. Each of them has some advantages and disadvantages (mainly the size):

RAW data are output data by the Event Filter (see previous Section) for reconstruction. The event size should be about 1.6 MB, arriving at an output rate of 200 Hz.

ESD (Event Summary Data) contains the detailed output of the detector reconstruction and is produced from the raw data. ESD has an object-oriented representation, and is stored in POOL ROOT files. The size of an event is about 1 MB per event.

AOD (Analysis Object Data) is a summary of the reconstructed event and contains sufficient information for common analyses. It contains physics objects and other elements of analysis interest. It is also stored in POOL ROOT files, and is derived form ESD. The target size is 100 kB per event.

DPD (Derived Physics Data) is an n-tuple-style representation of event data for end-user analysis and histogramming.

TAG data are event-level metadata - thumbnail information about events to support efficient identification and selection of interesting events to a given analysis. The average size is 1 kB per event.

SIM (SIMulated Event Data) refers to generated events. Particles' interactions with the detector and detector response are simulated. The storage technology is POOL ROOT files. They are large (up to 2 MB per event) because they usually contain all generated metadata.
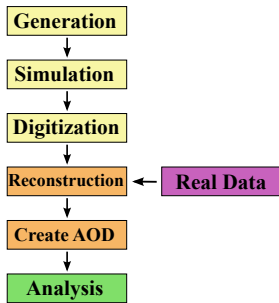

Figure 2.9: The ATHENA SW chain

Athena forms a software chain (see Fig. 2.9). The yellow boxes show full Monte Carlo production chain, orange describe steps needed to prepare data for analysis, purple box shows when the real data enter the chain and end-user analysis is shown in green box. Full chain (more detailed picture) can be found in Ref. [12].

Monte Carlo (MC) chain consists of Generation, Simulation and Digitization. Generators create an output of some physical process using MC generator that produces events with theoretically predicted probability. Example of an ATHENA integrated generator is Pythia or Herwig. A simulator takes a Lorentz 4-vector of a particle (created by generator) and adds the detector geometry and composition. As a result comes a collection of hits, which carry information like position, energy deposit, identifier of the active element etc. In the Digitization step the simulated hits are transformed so that they correspond to data coming from real detector (e.g. the response of the readout electronics and the imperfection of the detectors are taken in account). The output files coming from MC chain are Raw Data Objects (RDOs) and are resembling the real data from the detector.

The main task of the reconstruction is to transform RAW data into data usable for physics analysis which means to find hits, try to fit a track through them, and save it together with vertices, jets, missing energy etc. The output is stored in ESD and AOD formats.

During analysis, physicists interpret what happened in the real or simulated data. To do so there are several tools (only two will be mentioned):

ROOT

ROOT is an object-oriented framework written in C++. It can be used in an interactive or batch mode. ROOT was developed to quickly sort, access and analyse large data files. It can be used for example for histogramming and graphing to visualize and analyse distributions and functions, curve fitting (regression analysis), statistics and data analysis etc. ROOT is not ATLAS based programme, it is also employed in other experiments on the LHC, CERN or other laboratories all over the world.

Graphical tools

Histograms show statistical outcome from the data, but to view events a different programme must be used. At the ATLAS, Atlantis programme is used – a stand-alone Java application which uses simplified detector geometry. It is

used for the visual investigation and the understanding of the physics of single events.

Chapter 3

Data Analysis

In this chapter the data analysis that I have done in cooperation with the Prague J/ψ group will be described. It consists of study of the b quark productions mechanisms. The analysis measures angular correlation between two B mesons, which are required to decay into $J/\psi + X$ pairs and azimuthal angle correlation is then measured. Branching ratio for B meson to decay into $J/\psi + X$ is about 1%. Deep understanding of the J/ψ properties and ATLAS performance is required in order to perform this analysis which is still a work in progress.

3.1   The ATLAS Coordinate System

The ATLAS Coordinate System – as described in ATLAS WorkBook [13] – is defined as a right-handed system with the x-axis pointing to the centre of the LHC ring, the z-axis following the beam direction and the y-axis going upwards. In Point 1[1], positive z points towards Point 8 with a slope of -1.23%. The azimuthal angle $\phi = 0$ corresponds to the positive x-axis and ϕ increases clock-wise looking into the positive z direction. ϕ is measured in the range [-π, +π]. The polar angle θ is measured from the positive z axis. Pseudorapidity, η, is defined by

$$\eta = -\log\left(\tan\frac{\theta}{2}\right)$$

Transverse momentum, p_T, is defined as the momentum perpendicular to the LHC beam axis.

3.2   Muon Identification and Reconstruction

Muons identification and reconstruction in the ATLAS detector [14] covers a p_T range from 1 GeV to around 1 TeV and extends to $\mid \eta \mid < 2.7$. In muon analysis three categories of muons are recognized: *tagged*, *combined* and *standalone*.

---

[1]A common name given to the ATLAS's cavern.

They differ in where is their track recognised (description of ATLAS detector can be found in Chapter 2):

- The standalone muons come from reconstructed tracks in the Muon Spectrometer (MS). The track parameters are obtained from the MS track and are extrapolated to the interaction point. The standalone reconstruction covers $\mid \eta \mid < 2.7$.

- Muons from combined reconstruction are statistical combination of track parameters from both MS track and Inner Detector (ID) track. The combined reconstruction covers $\mid \eta \mid < 2.5$.

- Tagged muons are associated only with the ID track that is extrapolated to the MS. MS contains only a few hits, usually not enough to reconstruct a MS tracklet. The muon tagging covers $\mid \eta \mid < 2$.

Combined muons are best in terms of momentum resolution and purity. Tagged muons are usually used to compensate for lower detection and reconstruction efficiency in the areas of barrel-endcap transition region and they might be contaminated by the decays in flight of kaons and pions and hadronic punch-throughs.
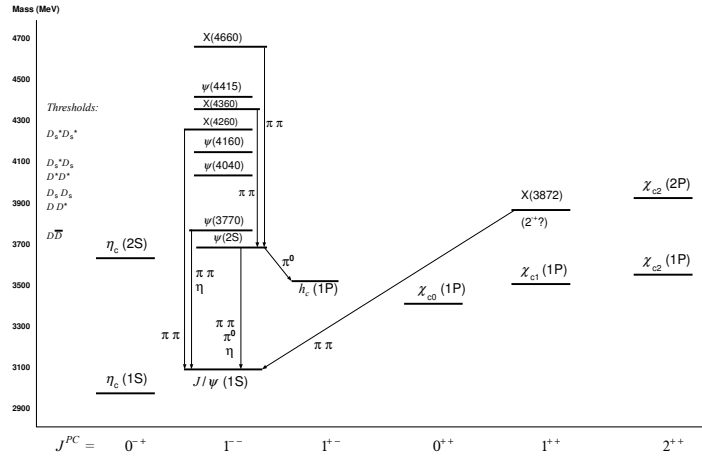
3.3 J/ψ Observation

Figure 3.1: The current state of knowledge of the charmonium system. Figure from [2]

Quarkonium is a bound state of a heavy quark and antiquark pair – in the case of charmonium they are charm and anticharm quark. Most famous charmonia example is the J/ψ meson whose properties are shown in Table 3.1.

Charmonium system is shown in Fig. 3.1. Quantum numbers are denoted by J^{PC} = notation where J stands for total angular momentum, P parity, and C charge conjugation. There are 8 bound states of charmonium: spin triplets $J/\psi(1S)$, $\psi(2S)$, $\chi_{c\ 0,1,2}(1P)$ and spin singlets $\eta_c(1S)$, $\eta_c(2S)$, $h_c(1P)$. Scalar states η_c can not decay into muons and are therefore harder to detect. The schema shows charmonia in the ground state (the vector J/ψ meson and pseudoscalar η_c) and in the excited state (the ψ' meson and three states of χ_c). All charmonium mesons above the $D\bar{D}$ threshold (slighly above $\psi(2S)$) decay predominantly into hadrons. Narrow width of J/ψ can be explained by the OZI rule (decay rates described by the Feynman diagrams with unconnected quark lines are suppressed).

J/ψ was discovered in 1974 by two independent experimental groups at BNL and SLAC. The BNL group was studying $p + Be$ collisions and SLAC group was studying e^+e^- annihilation. It was the first experimental confirmation of the fourth quark.

The J/ψ meson and its radially excited state ψ' (sometimes denoted as $\psi(2S)$) are states which are easily observed in the detector due to the large branching fraction of their dimuon decay channel.

Particle	Mass [Mev/c^2]	Width [Mev/c^2]	Decay mode	Branching ratio
J/ψ	3097	0.093	hadrons	87.7 ± 0.5
			e^+e^-	5.94 ± 0.10
			$\mu^+\mu^-$	5.93 ± 0.10
ψ'	3686	0.277	hadrons	97.9 ± 0.3
			$J/\psi + X$	56.1 ± 0.9
			e^+e^-	0.74 ± 0.18
			$\mu^+\mu^-$	0.73 ± 0.18

Table 3.1: Properties of J/ψ meson and its excited state ψ'. [2]

The aim of this analysis is to show that a J/ψ signal in the dimuon decay channel is strong and can be used in further analyses. To do so, specific algorithms and code were developed in cooperation with the Prague B-physics group. Dimuon is a special combination of muons: one muon and one antimuon $\mu^+\mu^-$. In my analysis I took all available muon data from 2011 ATLAS run (5.5 fb^{-1}) and selected events with at least two muons. Then I performed reconstruction of the invariant mass of the dimuon events (or combination of more dimuons in the event) which is shown in Fig. 3.2 and 3.3 in different mass ranges. In the first histogram, 3.2 J/ψ signal clearly dominates the mass spectrum. $\Upsilon(1,2,3)$ triplet is easily seen and at about 90 GeV the Z boson peak is clearly visible. Due to the dimuon production cross section it is not possible to record all dimuon events and they are being prescaled out by the trigger. To prevent throwing out of quarkonium events, B-physics dimuon triggers were implemented which select dimuon in the mass windows of J/ψ and $\Upsilon(1,2,3)$.

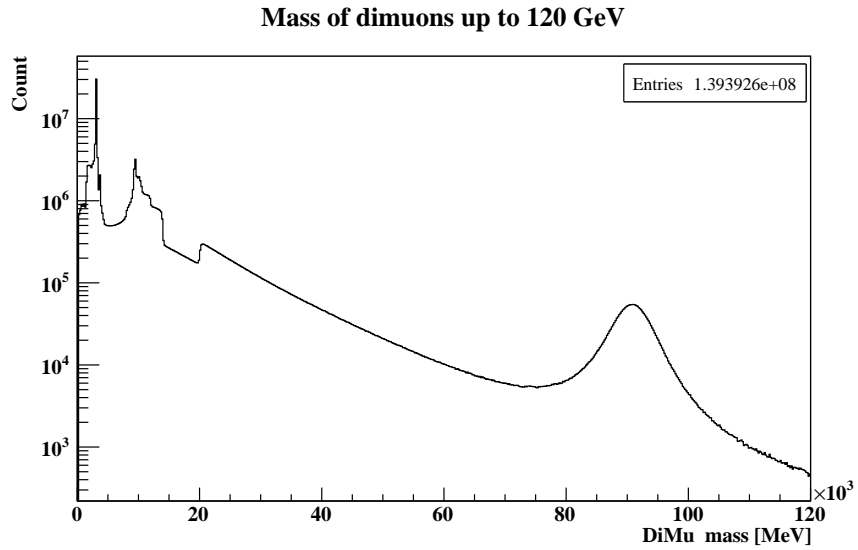Dips in the spectrum seen on Fig. 3.2 and 3.3 are caused by trigger prescales.

Mass of dimuons up to 120 GeV

Figure 3.2: Invariant mass plot of dimuons up to 120 GeV (log scale), 2011 data.

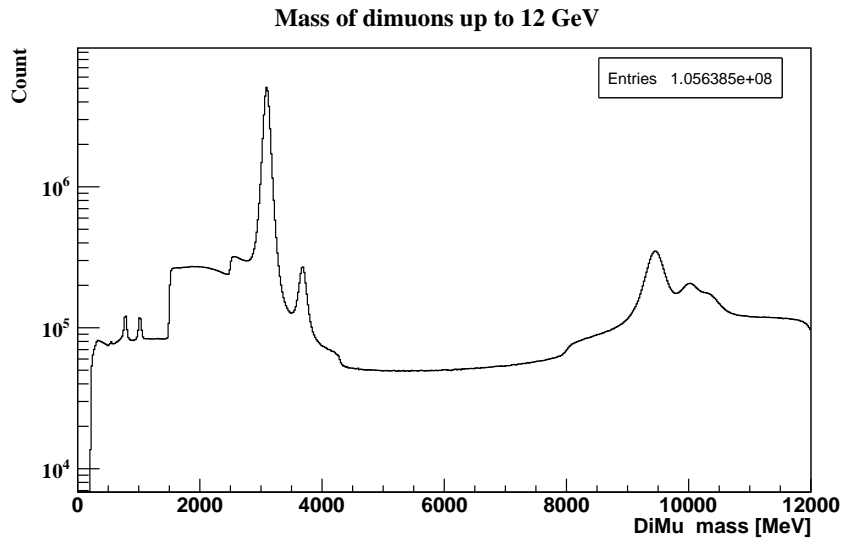**Mass of dimuons up to 12 GeV**

Figure 3.3: Invariant mass plot of dimuons up to 12 GeV in logarithmic scale.

The Invariant mass of the dimuons up to 12 GeV in both logarithmic and linear scales is shown in Fig. 3.3 and 3.4. On the logarithmic plot, we see a
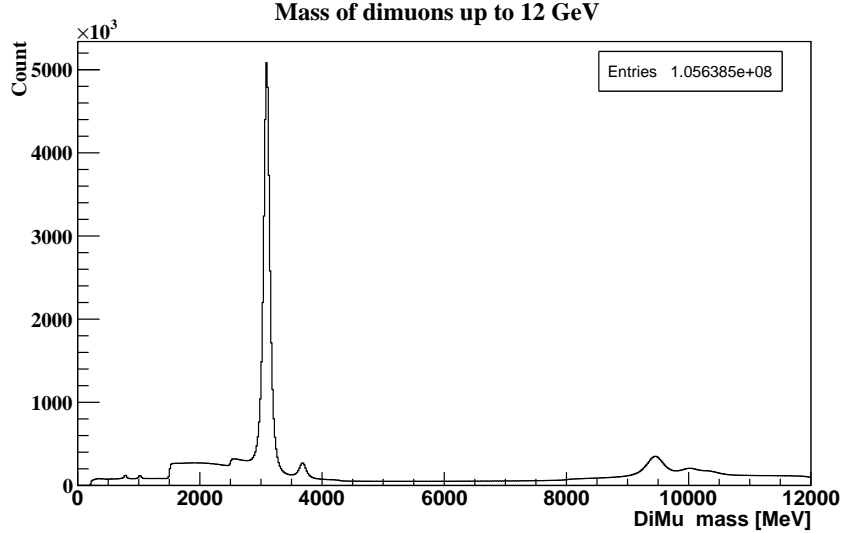
Figure 3.4: Invariant mass plot of dimuons up to 12 GeV in linear scale.

spectrum of vector meson resonances decaying into dimuon pair. At 782 MeV there is the narrow $\omega(782)$ resonance nearby the $\phi(1020)$, a bound state of $s\bar{s}$ quarkonium. At 3096 MeV there is a dominant J/ψ peak with about 14 million events. It's radial excitation, ψ' can be found next at 3686 MeV. The $\Upsilon(1,2,3)$ cascade is also distinguishable with clear peaks at 9460, 10023 and 10355 MeV respectively. While the width of the resonances is small, it is widened with the detector resolution. Mass difference between the upsilon states is comparable to the resolution of the detector and therefore they overlap. On the linear plot purity of the J/ψ signal can be seen. Main background sources under the J/ψ mass peak consists of random muons, chained semileptonic decays and decays in flight.

On hadron colliders, there are three production classes for J/ψ:

1. Direct production in QCD processes (also with contribution from electroweak processes),

2. Feed down from heavier charmonium states which account for about 40% of observed J/ψs,

3. Production in decays of B hadrons.

While the first and second case are almost indistinguishable, J/ψs born in B hadron decays can be easily selected. Lifetime of B hadrons (around 1.5 fs) allows them to fly away from the interaction point and decay. Vertex of their decay can be precisely reconstructed using tracks reconstructed by the Pixel detector.
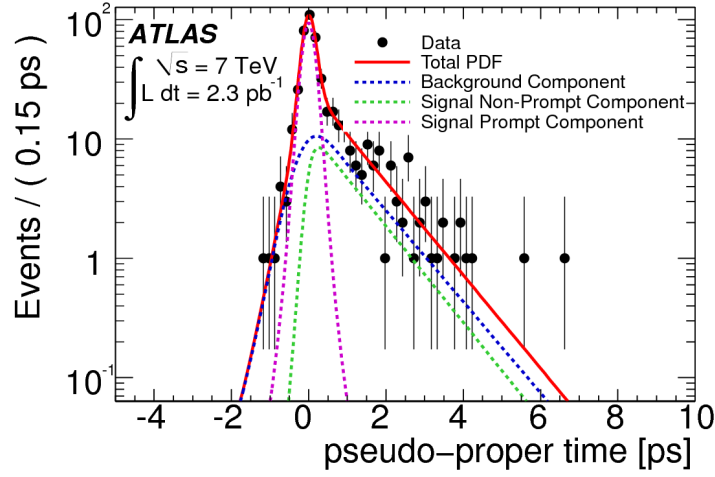
Figure 3.5: Pseudo-proper time distribution of $J/\psi \to \mu\mu$ candidates. Figure from [15]

A new variable, pseudo-proper lifetime is constructed for this purpose:

$$\tau = \frac{L_{XY} \cdot M_{J/\psi}}{p_T(J/\psi) \cdot c},\tag{3.1}$$

where L_{XY} denotes transverse flight length, $M_{J/\psi}$ the PDG mass of the J/ψ, p_T transverse momentum of the dimuon, and c stands for the speed of light.

Directly produced J/ψs have a pseudo-proper time close to zero whereas non-prompt J/ψ primarily come from B-hadron decays with an exponentially decaying pseudo-proper time distribution due to the lifetime of the parent B-hadrons. On the Fig. 3.5 an example of pseudo-proper lifetime is shown. Data are represented by a black points while total signal fit is red. Total pdf is made of signal plus background component. Signal is composed of indirect component represented by a Dirac delta distribution smeared with the detector resolution function modeled as a Gaussian, while indirect component is the exponential convoluted with the same detector resolution function. The significance (τ/σ_τ) greater than two is used to select indirect J/ψs.

In the analysis I have selected events which have contained at least 4 muons (2 positive and 2 negative) and events with at least 2 J/ψ candidates. Pairs of J/ψ candidates are shown on Fig. 3.6 where mass correlation of dimuon candidates clearly shows an excess of di-J/ψ events. Critical section is zoomed in on Fig. 3.7.
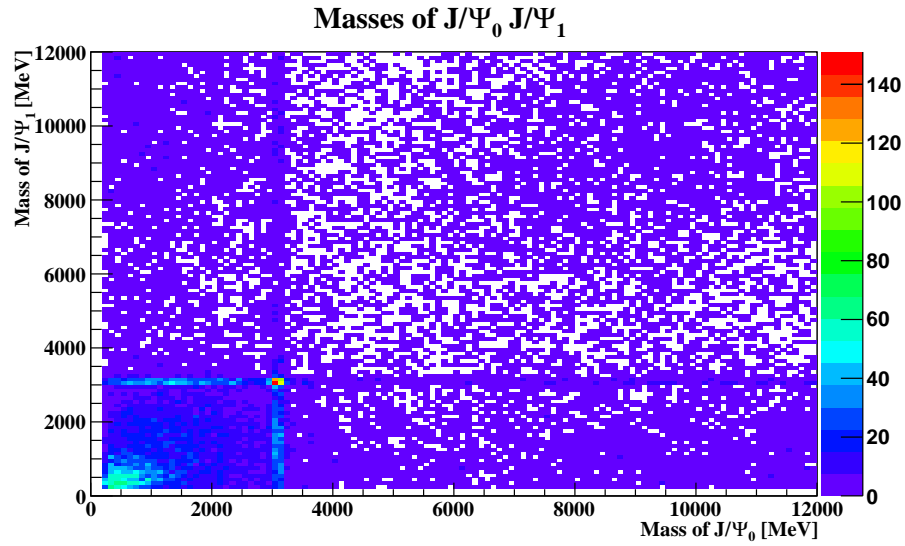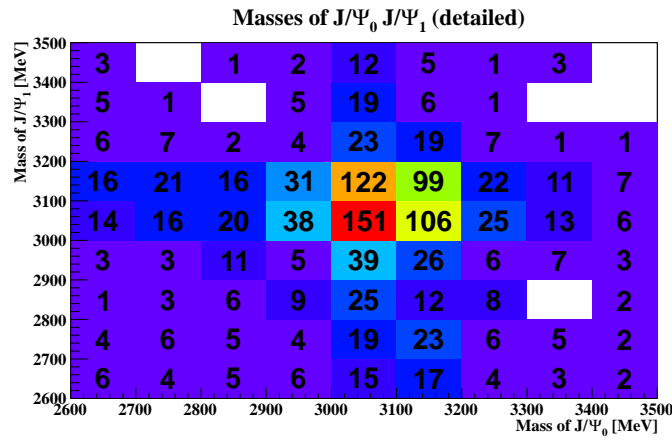
Figure 3.6: Mass correlation of two J/ψ candidates.

Figure 3.7: Detail of the mass peak signal.
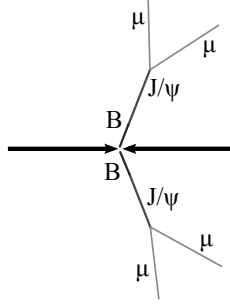
3.4 $b\bar{b}$ Angular Correlations

Figure   3.8:
Schematic view of
the $b\bar{b} \to J/\psi + J/\psi$
process

In this last section brief outlook of what use the previously analysed data can be. We have shown that the ATLAS detector has strong $J/\psi + J/\psi$ signal. This fact can be used in studying $b\bar{b} \to J/\psi + J/\psi$ decay which analyses $b\bar{b}$ angular correlations and thus the contributions from NLOQCD processes to the $b\bar{b}$ production (schematic view of the process can be seen in Fig. 3.8). Advantage of this channel for the study is the large mass of J/ψ meson. Firstly, $b\bar{b}$ pair is created in the proton-proton collision which then forms a B meson. B meson quickly decays into J/ψ (with a branching ratio of $\sim 1.1\%$) which then decays into two muons. B transfers huge part of its momentum to J/ψ because of its large mass therefore it is safe to say that the direction of flight was conserved and can be studied for $b\bar{b}$ production. Each of the production mechanisms described in Section 1.4.2 has different kinematic properties, which then enables us to decipher how the $b\bar{b}$ was produced. The differences are as follows:

Flavor creation
In FCR events b quarks are created during the hard scatter and have very high azimuthal distance $\Delta\phi$ (they emerge nearly back-to-back). They are well balanced in p_T.

Flavor excitation
In FEX events one of the quarks from $b\bar{b}$ pair gains a large transverse momentum due to the scattering and the other one travels collinearly with its parent gluon, therefore it has low p_T. The azimuthal distance $\Delta\phi$ is a broad distribution that is slightly suppressed at small angles.

Gluon splitting
In GSP events the $b\bar{b}$ pair is very close in phase space, since both tend to follow the direction of the gluon from the hard scatter interaction. Therefore $\Delta\phi$ peaks at small angles.

In Fig. 3.9 $b\bar{b}$ angular correlations simulated in PYTHIA [16] for LHC energies are shown. Green colour shows the GSP process, orange represents FEX process, whereas yellow color is FCR process. The distribution of the processes is clearly visible. On lower energies the contribution from GSP process is smaller and from back-to-back processes higher.

In Fig. 3.10 the preliminary results with 2011 data are shown. Solid lines show data with errors and the continuous line shows simulated data.

The advantage of using $b\bar{b} \to J/\psi + J/\psi$ channel is small background (e.g. no decays-in-flight, small number of chained semileptonic decays).
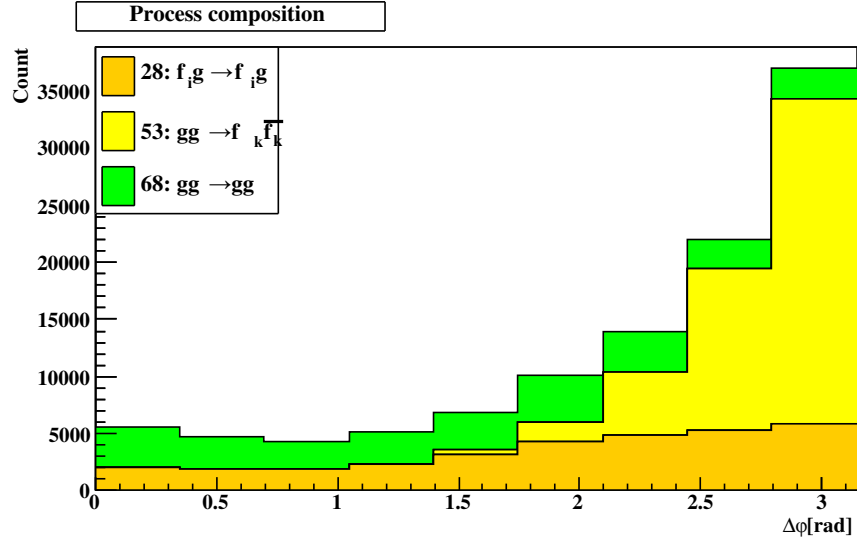
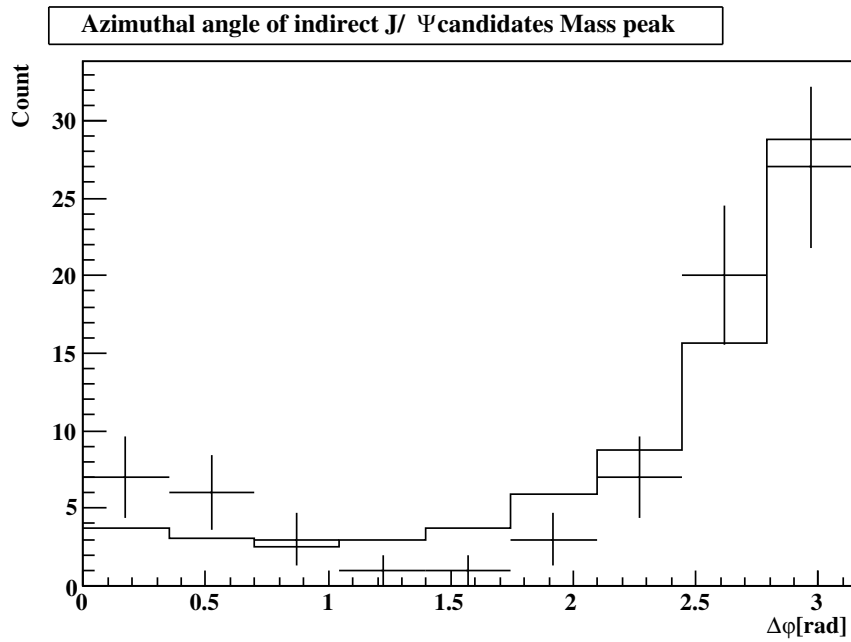Figure 3.9: PYTHIA simulated $b\bar{b}$ angular correlations.

Figure 3.10: $b\bar{b}$ angular correlation comparison of simulation to data.

All in all, preliminary results of this analysis seem promising, even though further study of this topic is required because measured data are not corrected for detector acceptance, trigger and reconstruction efficiency. This is the part where we will devote our effort and expect to finalize this analysis at the end of summer 2012.

Chapter 4

Thesis Summary

In this bachelor thesis a short overview of the particle physics and the Standard model is presented. A deeper explanation of physics of b quarks, their production mechanisms and J/ψ decay channels is given.

Second part of this thesis is devoted to the CERN laboratory, the LHC collider, its detectors and ATLAS in particular. Its subdetectors are discussed with the focus on the muon system and the Inner Detector.

Third part of this thesis concerns the data analysis in the muon stream. 2011 ATLAS data were used with accumulated statistics of about 5.5 fb^{-1} . Properties of J/ψ were studied in detail.

Main part of analysis, which is work in progress, is measurement of b quark production mechanisms using $B \rightarrow J/\psi + X$ decay channels for both B mesons. J/ψs coming from decay of the B hadrons can be selected using the pseudo-proper lifetime variable. We have found that there are about 500 Di-$J/\psi(\mu^+\mu^-)$ events in the 2011 data. To measure the angular correlations, template fit with PythiaB production mechanisms is performed on data. Data have to be corrected for the detector acceptance, trigger and muon efficiencies and this will be task I'm planning to work on this summer.

Bibliography

[1] D. Griffiths, *Introduction to Elementary Particles*. John Wiley & Sons, Ltd.

[2] K. Nakamura *et al.*, "Review of Particle Physics," *Journal of Physics G*, 2010.

[3] D. Perkins, *Introduction to High Energy Physics*. Cambridge University Press.

[4] "Cern press release: Cern experiments observe particle consistent with long-sought higgs boson. Communiqué de presse du cern : Les expériences du cern observent une particule dont les caractéristiques sont compatibles avec celles du boson de higgs tant attendu," p. 1, Jul 2012.

[5] L. Scudder, "Wikipedia commons." `http://commons.wikimedia.org/wiki/User:Laurascudder`, 31.5.2012.

[6] B. Martin, *Nuclear and Particle Physics*. John Wiley & Sons, Ltd.

[7] D. A. Wijngaarden, "Angular correlations in beauty production at the tevatron at $\sqrt{s} = 1.96$ tev," Master's thesis, Radboud University.

[8] The CERN collaboration, "Cern experiment public pages." `public.web.cern.ch/public/`, 31.5.2012.

[9] The ATLAS collaboration, "Atlas experiment public pages." `http://atlas.ch`.

[10] The ATLAS Collaboration, G. Aad, *et al.*, "The ATLAS Experiment at the CERN Large Hadron Collider," *JINST*, 2008.

[11] *ATLAS muon spectrometer: Technical Design Report*. Technical Design Report ATLAS, Geneva: CERN, 1997. distribution.

[12] The ATLAS collaboration, "Athena full chain." `https://twiki.cern.ch/twiki/bin/viewauth/Atlas/WorkBookFullChain`, 2012.

[13] The ATLAS Collaboration, "The atlas computing workbook." `https://twiki.cern.ch/twiki/bin/viewauth/Atlas/WorkBook`, 2012.

[14] "First observation of the $j/\psi \rightarrow \mu^+\mu^-$ resonance in atlas pp collisions at $\sqrt{s} = 7$ tev," Tech. Rep. ATLAS-CONF-2010-045, CERN, Geneva, Jul 2010.

[15] G. Aad *et al.*, "Measurement of the differential cross-sections of inclusive, prompt and non-prompt production in proton–proton collisions at," *Nuclear Physics B*, vol. 850, no. 3, pp. 387 – 444, 2011.

[16] T. Sjostrand, S. Mrenna, and P. Z. Skands, "PYTHIA 6.4 Physics and Manual," *JHEP*, vol. 0605, p. 026, 2006.